Nonlinear Dyn (2012) 67:2609–2619
DOI 10.1007/s11071-011-0174-4

ORIGINAL PAPER

On the transient response of forced nonlinear oscillators

Ryan J. Monroe · Steven W. Shaw

Received: 12 March 2011 / Accepted: 21 July 2011 / Published online: 8 September 2011
© Springer Science+Business Media B.V. 2011

Abstract We consider the transient response of a prototypical nonlinear oscillator modeled by the Duffing equation subjected to near resonant harmonic excitation. Of interest here is the overshoot problem that arises when the system is undergoing free motion and is suddenly subjected to harmonic excitation with a near resonant frequency, which leads to a beating type of transient response during the transition to steady state. In some design applications, it is valuable to know the peak value of this response and the manner in which it depends on system parameters, input parameters, and initial conditions. This nonlinear overshoot problem is addressed by considering the well-known averaged equations that describe the slowly varying amplitude and phase for both transient and steady state responses. For the undamped system, we show how the problem can be reduced to a single parameter χ that combines the frequency detuning, force amplitude, and strength of nonlinearity. We derive an explicit expression for the overshoot in terms of χ, describe how one can estimate corrections for light damping, and verify the results by simulations. For zero damping, the overshoot approximation is given by a root of a quartic equation that depends solely on χ, yielding a simple bound for the overshoot of lightly damped systems.

Keywords Nonlinear transient dynamics · Nonlinear overshoot · Harmonically forced Duffing oscillator · Duffing oscillator transients

R.J. Monroe (✉)
Air and Missile Defense Department, The Johns Hopkins University Applied Physics Laboratory, Laurel, MD, 20723 USA
e-mail: ryan.monroe@jhuapl.edu

S.W. Shaw
Department of Mechanical Engineering, Michigan State University, East Lansing, MI, USA

1 Introduction

Most studies of the response of nonlinear vibratory systems subjected to harmonic excitation focus on steady state response. Typical investigations consider periodic responses, stability, and bifurcations of these quasiperiodic responses, and chaotic responses. In this paper, we consider the transient response of the Duffing equation subjected to harmonic excitation, focusing on overshoot that occurs when the excitation is suddenly switched on. The Duffing oscillator is an archetypical nonlinear system that models many engineering systems [1, 2, 11, 12, 15, 27, 30, 32]. There exists a large body of work on the steady state response and its stability for this classical oscillator; see, for example, [27]. However, in certain design scenarios, it is useful to know the short-term transient dynamics of the response [23]. For instance, one may have design constraints on the peak amplitude of a system response, and the transient response amplitude may violate this constraint, even when the steady state amplitude does not. Such an application motivated the

present study, specifically, the response of a vibration absorber that starts in an inactive state and is suddenly brought into conditions for it to be active, leading to beating type transients. Another consideration is that a transient can sometimes result in the system ending up in an undesirable steady state, in situations where multiple stable steady state responses exist.

The approach for investigating the transient response of a linear oscillator is straightforward, since one can express the exact solution of the differential equation governing the system response in terms of the system and excitation parameters and initial conditions [14, 34, 37]. Another approach is to find a constant of motion for the system that relates the position, velocity, system parameters, and initial conditions, from which the peak response can be determined [5, 18, 19]. Both approaches provide exact analytical results for the transient response in the linear case. However, the constant of motion approach typically does not apply for nonautonomous systems. As for nonlinear systems, the direct solution approach can be used only in a few special cases [3], whereas the latter approach can be applied to a number of nonlinear systems [4, 9, 10, 29]. In addition, the constant of motion approach is well suited for problems such as determination of the overshoot, in which the velocity is given (zero in this case) at some desired system position (peak amplitude in this case). A limitation with the constant of motion approach is that it is not directly applicable to systems with time-dependent excitation. However, the method of averaging provides a mean of removing this time dependence for a certain class of systems, so that a constant of motion for the averaged system can be obtained [36]. That methodology is utilized here, and was also employed in a recent two-part paper describing an investigation of the same general problem considered here, namely, the transient response of the resonantly forced Duffing oscillator [21, 22]. The distinctions of the present results from those in [21, 22] are: (i) the focus on the nonlinear overshoot problem, which is not directly studied in [21, 22], and (ii) the scaling of the problem such that the undamped (damped) problem depends on one (two) parameter(s), χ (and D). The outcome of the present analysis is a very simple curve of the undamped ($D = 0$) system overshoot versus χ, which provides a useful bound for system with weak damping. Other work on transient dynamics of nonlinear oscillators includes applications of energy transfer and energy pumping in systems with strong nonlinearities [16, 28, 38, 39], and works on a variety of other, tangentially related, topics [8, 11, 13, 17, 20, 24, 31].

The primary focus here is an analytical treatment of the transient dynamics of the Duffing oscillator that allows for predictions of the nonlinear overshoot. The main result is a closed form expression for the overshoot for the case of zero damping when the system starts with zero amplitude initial conditions. It is shown that this undamped result provides a useful, conservative bound for system overshoot; one that is quite accurate for systems with light damping. The analysis is aided by a convenient scaling of the position and time such that the three system parameters, namely the force magnitude, frequency detuning, and nonlinearity, are combined into a single parameter χ. The predictive result is compared against simulations of the original nonlinear oscillator and the averaged equations to demonstrate its accuracy.

2 The model, averaged equations, and scaling

The system of interest here is a single degree-of-freedom oscillator with small damping, nonlinearity, and harmonic excitation, driven near resonance, expressed as

$$x'' + \omega_0^2 x = \epsilon\big(F\sin(\omega t + \phi) - \xi x^3 - \mu x'\big), \tag{1}$$

where ϵ is a small parameter. In order to apply the method of averaging, we use the standard change of coordinates,

$$\begin{aligned} x(t) &= a(t)\sin\big(\omega t + \psi(t)\big), \\ x'(t) &= a(t)\omega\cos\big(\omega t + \psi(t)\big), \end{aligned} \tag{2}$$

which will have slowly varying amplitude and phase when $\epsilon \ll 1$ and the forcing is near resonance, $\omega \approx \omega_n$. Constraining the response of (1) to be in the form (2), defining the frequency detuning as $\epsilon\sigma = \omega^2 - \omega_0^2$, and averaging over one period of the excitation, results in the following standard averaged equations:

$$r' = -\frac{\epsilon}{2\omega}\big(F\sin(\Phi) + \mu r\omega\big), \tag{3}$$

$$r\Phi' = \frac{\epsilon}{2\omega}\left(\frac{3}{4}\xi r^3 - F\cos(\Phi) - \sigma r\right), \tag{4}$$

where r is the averaged amplitude and $\Phi = \varphi - \phi$ is the relative phase between the averaged oscillator

phase φ and the phase of the forcing. In addition, since the forcing phase ϕ is constant, we have replaced φ' with Φ' in (4) for convenience in the subsequent analysis.

We reduce the number of system parameters by scaling the dependent variable r and the independent variable t as follows:

$$t = \left(\frac{4\omega}{\epsilon\sigma}\right)\tau, \qquad r = 2\left(\frac{F}{\sigma}\right)p, \tag{5}$$

where it is assumed that $\epsilon\sigma \neq 0$. Utilizing this scaling in (3) and (4) results in the rescaled averaged equations,

$$\frac{dp}{d\tau} = -\sin(\Phi) - Dp, \tag{6}$$

$$p\frac{d\Phi}{d\tau} = 4\chi p^3 - \cos(\Phi) - 2p, \tag{7}$$

where

$$\chi = \frac{3}{2}\xi\left(\frac{F^2}{\sigma^3}\right) \quad \text{and} \quad D = 2\left(\frac{\mu\omega}{\sigma}\right). \tag{8}$$

Note that this scaling introduces a complication of the results exactly at resonance, where $\sigma = 0$. However, it will be shown that this is not a limitation for the overshoot problem since the results can be computed in the limit $\sigma \to 0$. Also, it is important to note that when $\sigma < 0$ both position and time of the scaled system become negative, since $\epsilon > 0$ and $\omega > 0$. In this case, the system is solved in reverse time, which may lead one to think the system amplitude response will grow exponentially. However, the sign of the scaled damping coefficient depends on σ as well, such that solving in reverse time will result in exponential decay, as expected. In addition, the results presented subsequently are simplified by making use of the inherent symmetry in the hardening vs. softening Duffing responses, in such a manner that negative amplitude responses can be ignored. However, it will be shown that this symmetry between softening vs. hardening Duffing oscillators does not carry over to the phase response and, therefore, we will need to consider the individual cases for the phase response.

2.1 The steady-state response

The steady state response of the scaled system is obtained by letting $dp/d\tau = 0$ and $d\varphi/d\tau = 0$, which results in the following equations for the steady state amplitude $\bar{p}$ and phase $\bar{\Phi}$,

$$(D\bar{p})^2 + \left(4\chi\bar{p}^3 - 2\bar{p}\right)^2 = 1, \tag{9}$$

$$\tan\left(\bar{\Phi}\right) = \frac{-D}{4\chi\bar{p}^2 - 2}. \tag{10}$$

It is seen that this scaling has reduced the system parameter dependence of the steady state response from four (ξ, F, σ, μ) to two (χ, D). In general, one can solve (9) analytically to obtain six roots governing the steady state amplitude $\bar{p}$ as a function of D and χ. However, for plotting the steady state response, we use only the three positive roots, since the other three are symmetric with respect to $\bar{p} = 0$ and do not provide any additional information about the steady state amplitude. These roots are given explicitly in Appendix A. More specifically, the three ignored roots are negative, which for $\sigma < 0$ lead to a positive $\bar{r}$ (see (5)) that match the positive roots for $\bar{p}$ for $\sigma > 0$. It is also important to note that there is a symmetry in the steady state frequency responses of two Duffing oscillators wherein one is hardening (ξ_1) and the other is softening (ξ_2), such that $\xi_1 = -\xi_2$, with all other parameters fixed. As seen by the definition of χ, the frequency response of these two systems are symmetric about $\sigma = 0$, provided the other parameters are the same. When considering the steady state phase response, this symmetry does not exist, that is, $\bar{\Phi}_1 \neq \bar{\Phi}_2$ for $\sigma_1 = -\sigma_2$, as can be seen from (10), where the steady state phase depends on the sign of σ through the damping coefficient D. Therefore, in the scaled system, for a given value of D, one distinct steady state amplitude exists as χ is swept, an example of which is shown in Fig. 1(a). However, the steady state phase can take one of two forms, depending on the sign of D, which is governed by σ; these are shown in Figs. 1(b) and (c). As expected, Figs. 1(a), (b), and (c) exhibit the familiar bistable region over which three steady state responses exist for a single value of χ, two of which are stable. We refer to these in terms of "the lower branch" (labeled as **A**), "the middle branch" (labeled as **B**), and "the upper branch" (labeled as **C**), designated by their relative amplitudes. The bistable region is given by $\chi_1^\star < \chi < \chi_2^\star$, which depends on the damping coefficient D. Explicit formulas for $\chi_1^\star$ and $\chi_2^\star$ are given in Appendix A. For the case of zero damping ($D = 0$), the results simplify to $\chi_1^\star = 0$ and $\chi_2^\star = 8/27$.

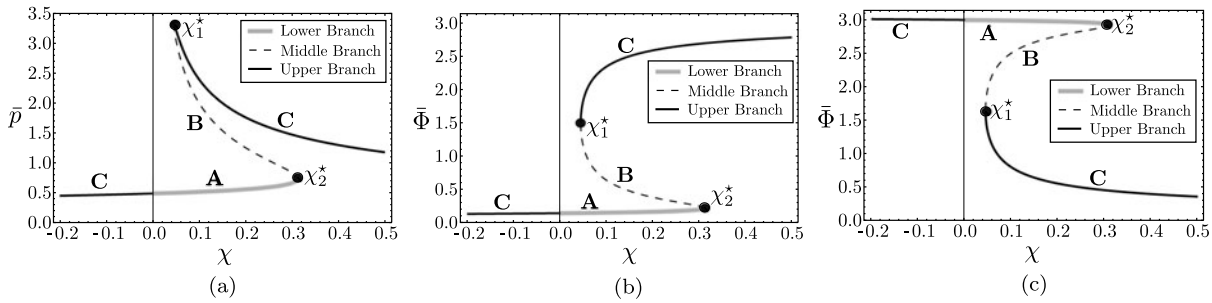

Fig. 1 Steady-state response of the scaled averaged system as a function of χ. (**a**) Steady-state amplitude for $|D| = 0.30$; (**b**) steady-state phase for $D = 0.30$, relevant for $\sigma > 0$; (**c**) steady-state phase for $D = -0.30$, relevant for $\sigma < 0$

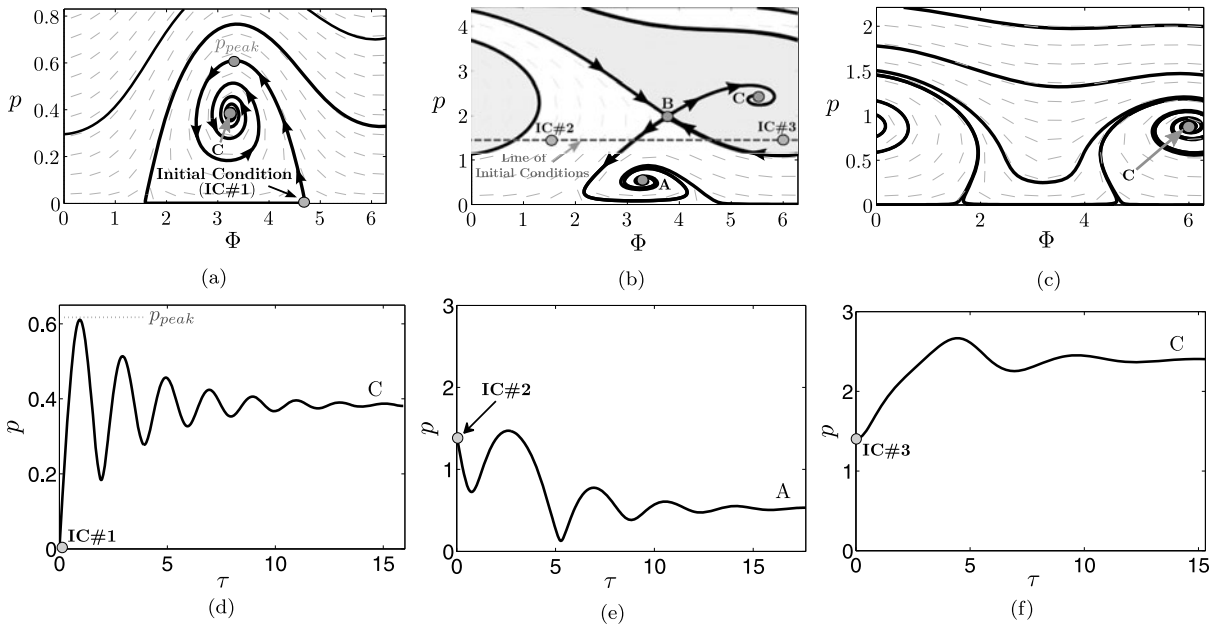

Fig. 2 Sample phase portraits and transient time traces for three values of χ, with $D = 0.30$. (**a**) Phase portrait for $\chi = -1 < \chi_1^\star$; (**b**) phase portrait for $\chi = 0.10 \in (\chi_1^\star, \chi_2^\star)$; (**c**) phase portrait for $\chi = 1 > \chi_2^\star$; (**d**) transient time response for zero amplitude initial conditions IC#1 for $\chi = -1$; (**e**) transient time response for $\chi = 0.10$ and initial conditions IC#2; (**f**) transient time response for $\chi = 0.10$ and initial conditions IC#3. Note that the initial amplitudes p_0 are the same for IC#2 and IC#3, but the different initial phases Φ_0 result in different steady state outcomes

2.2 The averaged equation phase portraits

The (p, Φ) phase portraits of the averaged equations are very useful for analyzing the transient trajectories of the Duffing equation [21, 22], and the remainder of the paper will make use of this information. In fact, for many of the results, we will focus on the undamped case, $D = 0$, since this case yields analytical solutions that provide a good approximation, and a useful bound, for lightly damped systems.

Figures 2(a)–(c) show phase portraits of a lightly damped system ($D = 0.30$) for three values of χ, displaying the three topologically distinct cases.[1] Attendant sample transient time responses are shown in Figs. 2(d)–(f) for the initial conditions (p_0, Φ_0) labeled as IC#1, IC#2, and IC#3. Figure 2(a) shows a sample phase portrait for $\chi < \chi_1^\star$. For this range of χ,

[1] Note that we have not shown the case when $D \neq 0$ and $\chi \in (0, \chi_1^\star)$, which is the case of the lower branch **A** existing alone. However, as seen from Figs. 1(a)–(c), this case will be qualitatively similar to the case of $\chi < 0$, which is shown in Fig. 2(a), except that the equilibrium point **C** is replaced with equilibrium **A**. Also, note that this case will not exist for $D = 0$.

only the upper branch (**C**) exists. Figure 2(d) depicts a sample transient time response for this case with initial condition IC#1, specifically, with zero amplitude, $p_0 = 0$. Since $p(\tau)$ describes the amplitude envelope of the oscillatory response with frequency near ω, the oscillation in p demonstrates the beating nature of the x response. Note that p and x both have a peak amplitude given by p_{peak}, and that p decays to the steady state amplitude $\bar{p}_C$ of branch (**C**). The more interesting phase portrait is for the bistable case, as shown in Fig. 2(b), for a value of $\chi \in (\chi_1^\star, \chi_2^\star)$. As depicted in the time responses shown in Figs. 2(e) and (f), depending on the initial conditions (p_0, Φ_0), generic transient trajectories approach either (**A**) or (**C**). The sample initial conditions shown have equal initial amplitudes and different initial phases, as indicated by IC#2 and IC#3 in Fig. 2. As usual, the basins of attraction for these two stable outcomes are separated by the stable manifold of the saddle point (**B**). Lastly, Fig. 2(c) shows a sample phase portrait for $\chi > \chi_2^\star$, for which **C** is the only possible steady state.

We now turn to an analysis that offers predictive results for the peak of the transient response.

3 Percent overshoot for the undamped system

In this section, an analytical result for the percent overshoot for the undamped Duffing oscillator is derived. In general, the percent overshoot of a system is defined as

$$\%\ Overshoot = \left(\frac{p_{max} - p_{ss}}{p_{ss}}\right) \times 100, \tag{11}$$

where p_{max} is the peak amplitude during a transient response and p_{ss} is the resulting steady state amplitude (given by one of the roots $\bar{p}$). Our analysis follows in a general manner the methods presented in [21, 22], adapted to focus on the overshoot question, and expressed here in terms of χ. We begin by deriving an energy-like constant of motion for the undamped ($D = 0$) scaled averaged equations. This is a fourth-order polynomial in p whose roots dictate the important features of the transient response. These roots are a function of the initial conditions (p_0, Φ_0), the parameter χ, and the relative phase of the response Φ. It will be shown that the peak amplitude of the response occurs at a relative phase of either $\Phi = 0$ or $\Phi = \pi$, so that the roots can be expressed in terms of the initial conditions and χ. One feature of interest will be the case where the transient response approaches the saddle point **B** for $\chi \in (\chi_1^\star, \chi_2^\star)$, since this will represent the basin boundary in the bistable case.

3.1 Transient response amplitudes

The averaged equations (6) and (7) with $D = 0$ is conservative and has a constant of motion that can be determined by combining (6) and (7) into a differential equation for $p(\Phi)$. Integrating this exact equation leads to the following integral of motion:

$$-\chi p^4 + p^2 + p\cos(\Phi) = c_1, \tag{12}$$

where c_1 is an arbitrary constant determined by the initial conditions (p_0, Φ_0) and χ. Equation (12) allows one to construct the phase portrait for the conservative averaged system in the usual manner: Given initial conditions (p_0, Φ_0) one can obtain c_1 and then solve (12) for phase plane trajectories in the form $p(\Phi)$ (or, simpler in this case $\Phi(p)$, since it has only two branches). An example phase portrait is shown in Fig. 3 for $\chi = 0.066 \in (\chi_1^\star, \chi_2^\star)$, which is an undamped version of the phase portrait shown in Fig. 2(b).

In general, (12) will have four roots for p that can be obtained exactly and will generate the level curves shown in Fig. 3; these roots are presented in Appendix C. In order to generate the level curves shown in Fig. 3, as well as the level curves when χ is outside of the bistable region, one needs only three of the four roots. Furthermore, it turns out that only two of these roots involve trajectories that include the peak amplitude about the steady state equilibria and, therefore,

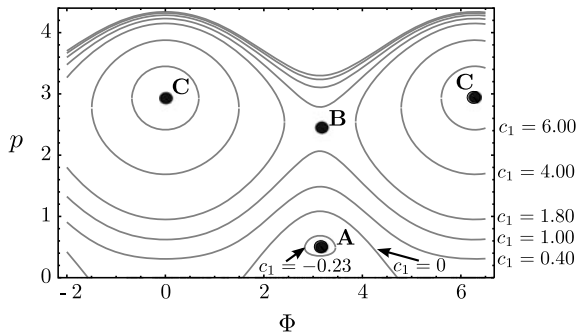

Fig. 3 Phase plane plotted using level curves of (12) by varying c_1, for $\chi = 0.066$ and $D = 0$

the other two roots are ignored for the present study. The two roots governing the transient trajectories of interest are given in (23) and (24) in Appendix C. Given a value of χ in the bistable region, and initial conditions (p_0, Φ_0), the root p_1 (23) will generate a transient trajectory as a function of Φ about the steady state equilibrium **A**. On the other hand, for any value of χ and initial conditions (p_0, Φ_0), the root p_2 (24) will generate a transient trajectory as a function of Φ about the steady state equilibrium **C**.

These results provide an analytical expression for the percent overshoot of the undamped Duffing oscillator. For χ in the bistable region, the peak amplitude of transient trajectories approaching branch **A** (branch **C**, respectively) can be determined by evaluating the root p_1 (p_2, respectively) at $\Phi = \pi$ ($\Phi = 0$, respectively). Outside the bistable region, the transient peak amplitude about the upper branch **C** can be determined by evaluating root p_2 at $\Phi = \pi$ when $\chi < \chi_1^\star = 0$, and at $\Phi = 0$ for $\chi > \chi_2^\star = 8/27$.[2] Note that for a negative initial amplitude condition $p_0 < 0$, corresponding to $\sigma < 0$ according to (5), the determination of the peak amplitude p_{max} is slightly modified, the details for which are given in Appendix B.

To determine the percent overshoot, the steady state amplitudes for **A** and **C** are also required. These can be determined as a function of χ by solving (9) for $\bar{p}$, using the analytical expressions given in Appendix A (15)–(16) evaluated at $D = 0$. From the peak and steady state amplitudes, the percent overshoot can be computed in an explicit form. This result is rather cumbersome, due to the roots involved, and is therefore not given explicitly, but it is straightforward to compute.

3.2 Basin separation trajectory

It is also of use to determine the location of the saddle point **B** (see (17)), since this, along with the attendant transient trajectories, determines basin boundaries for steady-state fixed points **A** and **C**. This information is useful if it is desired to have a system reach a particular steady state when operating in the bistable region.

[2]Although we have not shown the undamped portraits when χ is outside the bistable region, the interested reader can refer to the damped phase portraits shown in Figs. 2(a) and (c) to clarify where Φ is evaluated.

To begin, we first derive the initial conditions that will result in a transient trajectory on the stable or unstable manifolds of **B** when $D = 0$. This is done by evaluating the initial conditions for (12) at the steady state amplitude $p_0 = p_B$ and phase $\Phi_0 = \pi$, resulting in the following condition on (25),

$$\begin{aligned} c_1^\star(\chi) &= c_1(\chi, p_B, \pi) \\ &= \frac{1}{288\chi^3}\Big(4\chi(3\nu)^{2/3} + 192^{1/6}\delta\nu^{1/3}\Big(\frac{9}{2}\nu^{1/3} \\ &\quad - 3^{2/3}\Big) + 3\chi^2\big(16 - 18(3\nu)^{1/3} \\ &\quad + 9(3\nu)^{2/3}\big)\Big), \end{aligned} \tag{13}$$

where

$$\begin{aligned} \nu &= \delta\sqrt{3} - 9\chi^2, \\ \delta &= \chi^{3/2}\sqrt{27\chi - 8}, \end{aligned} \tag{14}$$

for $\chi \in (0, 8/27)$. One can now use $c_1^\star$ in the expressions for p_1 and p_2 to generate stable and unstable manifolds, as shown in Figs. 4(a)–(c). The trajectory of particular interest is the stable manifold, which is obtained from $c_1^\star$ in the expression for p_1 (23).

In general, these undamped basin boundaries provide a good approximation for the basin boundaries of the lightly damped system near **B**. These results can be used as follows: Suppose that the steady state at **A** is desired for all initial phases, then the maximum initial amplitude allowed is given by $p_{cr} = p_1(\chi, 0, c_1^\star)$, as indicated by the horizontal lines in Figs. 4(a) and (b) for two different values of χ. Note that for $\chi \in (4/27, 8/27)$, no such p_{cr} exists, since at $\chi = 4/27$ the homoclinic orbit to **B** changes character such that all small amplitude initial conditions lie in the basin of **C**, an example of which is shown in Fig. 4(c).

3.3 Numerical examples

In this section, two examples are shown to illustrate the main overshoot results, and the benefits of introducing the parameter χ. Although these examples consider only the case of zero initial amplitude ($p_0 = 0$, $\Phi_0 \in [0, 2\pi)$), corresponding to $c_1 = 0$, results for any initial conditions can be obtained by varying c_1. The first example compares the percent overshoot for systems with three different sets of original system parameters (F, ξ, σ) that all yield the

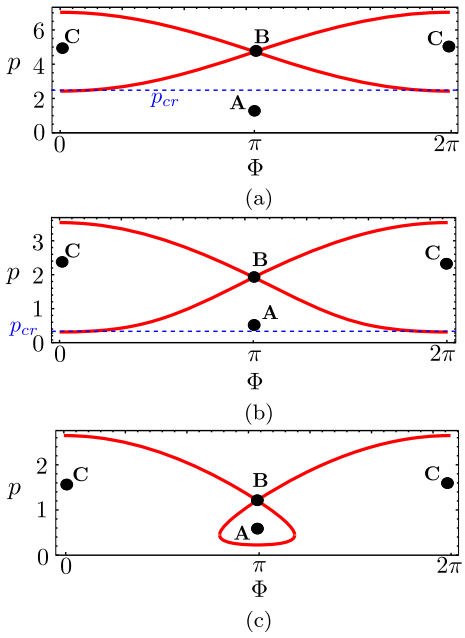

Fig. 4 Stable and unstable manifolds of **B** for three values of χ. (**a**) $\chi = 0.02$; (**b**) $\chi = 0.10$; (**c**) $\chi = 0.20$. (**a**) and (**b**) show lines of constant amplitude p_{cr}, which indicate the maximum amplitude of initial conditions p_0 such that the response will approach the lower branch for all values of the initial phase Φ_0. The topology of the homoclinic orbit about **A** changes from (**a**), (**b**) to that of (**c**) for $\chi > 4/27$. It is seen that for $\chi \in (4/27, 8/27)$, small amplitude initial conditions will result in a large amplitude steady state **C**, for all initial phases

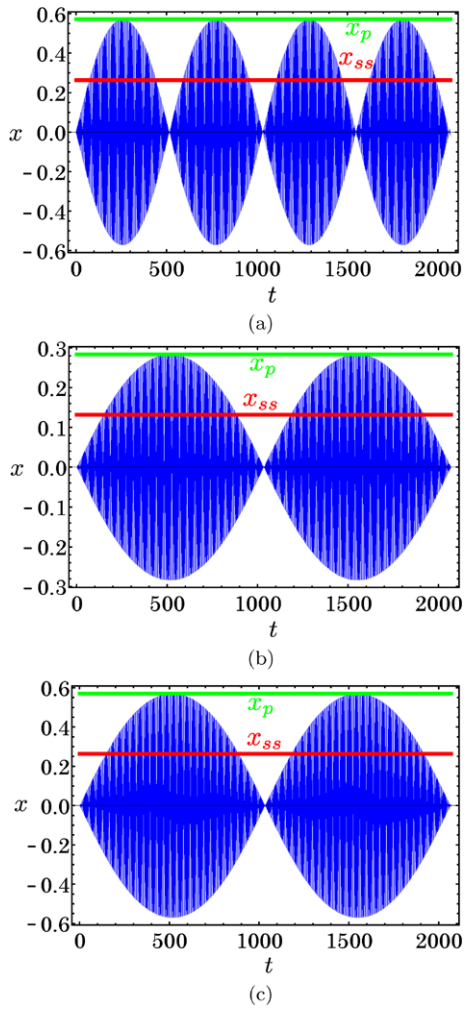

Fig. 5 Numerical simulations of (1) for $\epsilon = 0.03$ and $\omega = 2$, and three sets of system parameter values that yield $\chi = 0.094$, with a predicted overshoot of 115.8%. (**a**) $F = 1/2$, $\sigma = 2$, $\xi = 2$, simulated percent overshoot = 116.6%; (**b**) $F = 0.125$, $\sigma = -1$, $\xi = -4$, simulated percent overshoot = 115.3%; (**c**) $F = 0.177$, $\sigma = 1$, $\xi = 1$, simulated percent overshoot = 116.1%

same value of χ, and thus the same percent overshoot. The second example shows how the percent overshoot varies as a function of χ in the bistable region. Both examples show the percent overshoot relative to the lower branch **A**, since this is the resulting steady state for $p_0 = 0$ when $\chi < 4/27$. However, in the second example, for $\chi > 4/27$ and $\chi < 0$, the zero amplitude initial conditions result in a percent overshoot relative to **C**.

For the case of zero amplitude initial conditions ($c_1 = 0$) and zero damping ($D = 0$), the percent overshoot is a function of χ only. Figures 5(a)–(c) show simulations of the original equation (1) for three different sets of system parameter values that each give $\chi = 0.094$. The overshoot is calculated using the explicit expressions for the peak and steady state amplitudes for response **A** in (11); these expressions are (15), from Appendix A for the steady state amplitude, and (23) evaluated at $\Phi = \pi$ for the peak amplitude, from Appendix C. The result for $\chi = 0.094$ is a predicted percent overshoot of 115.8%. This prediction is compared with the results from direct simulations of (1), which are indicated in the figure caption, showing the accuracy of the results. Note that the differences in system parameters result in differences in the response amplitudes and the transient beat frequencies, but the percent overshoot is essentially identical in all three cases, as predicted.

We now consider how the percent overshoot resulting from zero amplitude initial conditions depends on χ. The analytical results are shown in Fig. 6(a), where the overshoot relative to branch **C** is shown

by the gray curves and those relative to branch **A** are shown by the black curve. Note that the percent overshoot for a linear undamped system is 100%, and there is transition at $\chi = 0$ from percent overshoot values less than 100% to those larger than 100%. Due to the nature of χ, this can be interpreted in various ways. For example, the overshoot for a hardening system ($\xi > 0$) driven below resonance ($\sigma < 0$) will be less than 100% and it can go only to **A**, while that for a softening system ($\xi < 0$) driven below resonance ($\sigma < 0$) will be greater than 100% in its transition to **A**. Note that the maximum possible overshoot is 173%, for softening systems with χ just below $\chi^* = 4/27$. The transition at χ^* corresponds to the case when the zero amplitude initial trajectory is on the stable manifold of **B**. For $\chi > \chi^*$, zero amplitude initial conditions result in transient trajectories headed toward **C**, and in this case the percent overshoot is less than 100%, since the amplitude of **C** is significantly larger than that of **A**. Lastly, note that as $\chi \to \pm\infty$ the percent overshoot is asymptotic to the limiting value of 58.74%, which corresponds to the percent overshoot at resonance, $\sigma = 0$, for branch (**C**).

Figure 6(b) shows a comparison of the analytical results (shown in Fig. 6(a)) and simulations of both the original Duffing equation (1) and the averaged equations (6) and (7), for the case of zero amplitude initial conditions. These results demonstrate the accuracy of the analytical method, and how it degrades as one increases the value of ϵ.

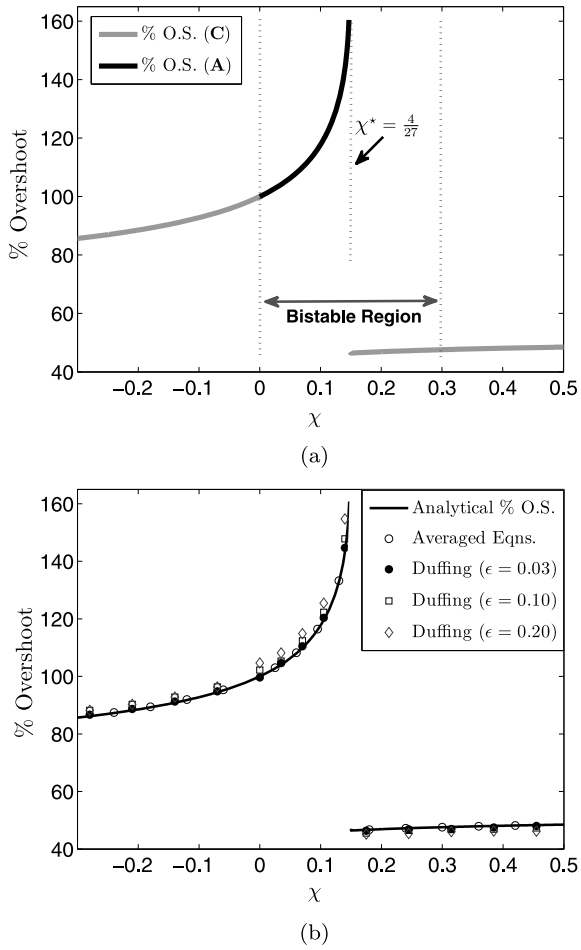

Fig. 6 (**a**) The analytical results for percent overshoot versus χ for zero amplitude initial conditions. The percent overshoot is computed relative to either the upper branch **C**, shown by the *solid gray curves*, or the lower branch equilibria **A**, shown by the solid black curve, depending on χ, as indicated in the inset. At $\chi = 4/27$, zero amplitude initial conditions results in a trajectory on the stable manifold of **B**. When $\chi < 0$ or $\chi > 4/27$, zero amplitude initial conditions results in transient trajectories about equilibria **C**, as shown in Fig. 4(c). Note that the phase at which (24) is evaluated to obtain p_{max} for the percent overshoot is different for $\chi < 0$ and $\chi > 4/27$, as described in Sect. 3.1. (**b**) Comparison of the analytical solution and simulations of both the Duffing oscillator (1) and the averaged equations (6) and (7) for the case of zero amplitude initial conditions and different values of ϵ. Parameter values used in the simulations are $F = 1/2$, $\sigma = 1.75$, and $\omega = 2$, and the nonlinearity ξ is varied from -4 to 7 to sweep the χ domain shown. It is noted that the percent overshoot is asymptotic to 58.74% as $\chi \to \pm\infty$ (i.e., as one approaches resonance, $\sigma \to 0$)

4 Conclusions

We have derived an approximate analytical method for predicting the overshoot for the transient response of a weakly nonlinear Duffing oscillator that is harmonically forced near resonance. The method makes use of the system's averaged equations, which yield an integral of motion in the undamped case, by which the system parameters and initial conditions can be related to the amplitude and phase of the system response. The resulting equation for the amplitude is a fourth-order polynomial, which can be solved as function of the response phase, system parameters, and initial conditions. This gives analytical expressions with parameter dependence for the amplitude response, with useful information about the peak amplitude, and for bistable systems, the ultimate steady state response achieved. A unique scaling reduces the problem to two parameters, χ, that combines the force magnitude F, the frequency detuning σ, and the nonlinearity ξ, and

D, which involves damping. Thus, the undamped results, which provide a useful bound for the overshoot in lightly damped systems, depend on a single parameter. Of course, the presence of damping will alter these results. A correction for small D has been computed, but is not shown here, as the payoff is small in comparison with the extensive nature of the calculations [25]. It seems to be more efficient to simply obtain the damped overshoot by simulating the damped average equations. These results build on, and complement, those of a recent similar study [21, 22], by focusing on the prediction of overshoot and formulating the problem in a manner that reduces the number of system parameters.

The results presented here are being used to predict overshoot for centrifugal pendulum vibration absorbers, which, in some applications, are activated when suddenly subjected to near resonant excitation [26, 34]. These absorbers must be designed to not exceed specified amplitudes, even during startup, and so transient predictions such as those derived here are of great practical value. For the case of tautochronic absorbers [6, 7, 33, 35], the system nonlinearities are much more complicated than the cubic term in the Duffing equation, yet we have shown that their averaged equations are integrable in the undamped case, so that similar predictive results can be achieved for that system [26]. Furthermore, this percent overshoot approach has also been applied to the case of parametric resonance and it has been found to produce simpler formulas for the overshoot than those given here. In fact, for the case of near zero amplitude initial conditions (i.e., $p_0 \approx 0$) it is remarkably found that the percent overshoot is simply $100(\sqrt{2}-1)$, and is therefore independent of the system parameters contained. These results include experimental evidence of the constant overshoot for near zero amplitude initial conditions, as well as an outline for computing the overshoot for nonzero amplitude initial conditions [25]. These extensions suggest that the approach may be quite general for weakly nonlinear systems of a more general form, and quite possibly for classes of conservative strongly nonlinear systems with periodic excitation.

Acknowledgements This work was supported by NSF grant CMMI-0700307 and by the Chrysler Challenge Fund. The authors are grateful to Brendan Vidmar, Brian Feeny, Nick Miller, Alan Haddow, and Bruce Geist for fruitful discussions.

Appendix A: Steady-state amplitudes

The steady state amplitudes for branch **A**, branch **C**, and saddle branch **B** are given by three of the six possible roots to (9) when $\chi \neq 0$. The three roots are as follows:

$$p_A(\chi, D) = \frac{1}{\sqrt{3\chi}}\sqrt{1+\frac{1}{8}\big(1+i\sqrt{3}\big)\big(3D^2-4\big)\lambda^{-1/3}+\frac{1}{8}\big(1-i\sqrt{3}\big)\lambda^{1/3}}, \tag{15}$$

$$p_C(\chi, D) = \frac{1}{\sqrt{3\chi}}\sqrt{1+\frac{1}{4}\big(4-3D^2\big)\lambda^{-1/3}+\frac{1}{4}\lambda^{1/3}}, \tag{16}$$

$$p_B(\chi, D) = \frac{1}{\sqrt{3\chi}}\sqrt{1-\frac{1}{8}\big(1-i\sqrt{3}\big)\big(3D^2-4\big)\lambda^{-1/3}-\frac{1}{8}\big(1+i\sqrt{3}\big)\lambda^{1/3}}, \tag{17}$$

where

$$\lambda = 2\big(27\chi-4-9D^2\big)+3\sqrt{3}\sqrt{D^6+8D^2\big(D^2+2-9\chi\big)+4\chi(27\chi-8)}. \tag{18}$$

The root p_C is valid for all values of $\chi \neq 0$. The roots p_A and p_B are valid in the bistable region $\chi \in (\chi_1^\star, \chi_2^\star)$. This range is determined by the conditions on χ for these roots to be real, specifically,

$$\chi_1^\star = \frac{1}{54}\Big(8+18D^2-\sqrt{\big(4-3D^2\big)^3}\Big), \tag{19}$$

$$\chi_2^\star = \frac{1}{54}\left(8 + 18D^2 + \sqrt{\left(4 - 3D^2\right)^3}\right). \tag{20}$$

For the undamped system results, roots are simply evaluated at $D = 0$. The linear ($\xi = 0,\ \chi = 0$) steady state forced response steady is recovered from (9), and is given by $\bar{p} = \frac{1}{\sqrt{4+D^2}}$.

Appendix B: Transient response symmetry

Similar to the steady state amplitude response, the transient amplitude response also possesses a symmetry that allows one to use the derived results to capture the case when $p < 0$, which arises when $\sigma < 0$ in the rescaled system. To see this, substitute $p = -k$ into (12) to obtain

$$-\chi k^4 + k^2 - k\cos(\Phi) = c_1, \tag{21}$$

which, upon replacing Φ with $\Phi + \pi$, one obtains

$$-\chi k^4 + k^2 + k\cos(\Phi) = c_1, \tag{22}$$

which is the same as (12). Therefore, the transient trajectories for $p < 0$ are the same as those for $p > 0$ with a phase shift of $\Phi + \pi$. The percent overshoot results for $p_0 < 0$ are obtained by computing c_1 using initial conditions ($|p_0|,\ \Phi_0 + \pi$). The resulting c_1 is then used in the roots given in (23) and (24) to find the peak amplitude p_{max} for the overshoot calculation.

Appendix C: Undamped transient response amplitudes

Here, we give the full analytical results needed for the percent overshoot calculation given in (11). The percent overshoot calculation uses the peak transient amplitude and the steady state amplitude for a given χ and initial conditions (p_0, Φ_0). The two roots of the transient equation (12) that contain the peak amplitudes about steady states **A** and **C**, as explained in the text, are given by,

$$p_1(\chi, \Phi, c_1) = \frac{1}{2\sqrt{3\chi}}\left(\sqrt{2+\kappa} - \left(4 - \kappa + \frac{6\sqrt{3\chi}\cos(\Phi)}{\sqrt{2+\kappa}}\right)^{1/2}\right), \tag{23}$$

$$p_2(\chi, \Phi, c_1) = \frac{1}{2\sqrt{3\chi}}\left(\sqrt{2+\kappa} + \left(4 - \kappa + \frac{6\sqrt{3\chi}\cos(\Phi)}{\sqrt{2+\kappa}}\right)^{1/2}\right), \tag{24}$$

where κ is

$$\kappa = \beta\left(\frac{2}{\alpha}\right)^{1/3} + \left(\frac{\alpha}{2}\right)^{1/3},$$

and β and α are defined as follows:

$$\beta = 1 + 12c_1\chi,$$

$$\alpha = \gamma + \sqrt{\gamma^2 - 4\beta^3},$$

$$\gamma = 9\chi\left(3\cos^2(\Phi) + 8c_1\right) - 2.$$

The constant c_1 is determined by the initial conditions (p_0, Φ_0) and χ, specifically,

$$c_1(\chi, p_0, \Phi_0) = -\chi p_0^4 + p_0^2 + p_0\cos(\Phi_0). \tag{25}$$

The roots p_1 and p_2 give transient trajectories as a function of the relative phase Φ, and for $D = 0$ the peak occurs at $\Phi = 0$ or $\Phi = \pi$, depending on the system parameters χ and the initial conditions (p_0, Φ_0). With the transient amplitude roots given here and the steady state amplitude roots given in Appendix A, one can formulate the percent overshoot about equilibria **A** and **C** by following the procedure given in Sect. 3.1.

References

1. Alsuwaiyan, A.S., Shaw, S.W.: Performance and dynamic stability of general-path centrifugal pendulum vibration absorbers. J. Sound Vib. **252**(5), 791–815 (2002)
2. Bajaj, A.K., Johnson, J.M.: On the amplitude dynamics and crisis in resonant motion of stretched strings. Philos. Trans. R. Soc., Math. Phys. Eng. Sci. **338**, 1–41 (1992)

3. Boyce, W., DiPrima, R.: Elementary Differential Equations and Boundary Value Problems. Wiley, New York (2000)
4. Chandrasekar, V.K., Senthilvelan, M., Lakshmanan, M.: On the complete integrability and linearization of certain second-order nonlinear ordinary differential equations. Proc. R. Soc. Lond. Ser. A, Math. Phys. Sci. **461**, 2451–2476 (2005)
5. Chandrasekar, V.K., Senthilvelan, M., Lakshmanan, M.: On the lagrangian and hamiltonian description of the damped linear harmonic oscillator. J. Math. Phys. **43** (2007)
6. Chao, C.P., Lee, C.T., Shaw, S.W.: Non-unison dynamics of multiple centrifugal pendulum vibration absorbers. J. Sound Vib. **204**(5), 769–794 (1997)
7. Chao, C.P., Shaw, S.W., Lee, C.T.: Stability of the unison response for a rotating system with multiple tautochronic pendulum vibration absorbers. J. Appl. Mech. **64**, 149–156 (1997)
8. Clauser, F.H.: The transient behavior of nonlinear systems. IRE Trans. Circuit Theory **7**, 446–458 (1960)
9. Denman, H.H.: Approximate invariants and lagrangians for autonomous, weakly non-linear systems. Int. J. Non-Linear Mech. **29**, 409–419 (1994)
10. Denman, H.H.: Approximate invariants and lagrangians for autonomous, weakly non-linear systems—ii. Linear friction. Int. J. Non-Linear Mech. **33**, 301–314 (1998)
11. D'Souza, M., Kumar, A., D'Souza, R.: Non-linear resonant transient and steady-state response in a classical model. J. Mod. Opt. **28**, 1039–1050 (1981)
12. Eckhardt, D.H.: A nonlinear analysis of the moon's physical libration in longitude. The Moon **2**, 309–319 (1971)
13. Gelb, A., Velde, W.E.V.: Multiple-Input Describing Functions and Nonlinear System Design. McGraw-Hill, New York (1968)
14. Hartog, J.P.D.: Mechanical Vibrations. Dover, New York (1985)
15. Hill, D.F.: Transient and steady-state amplitudes of forced waves in rectangular basins. In: 16th ASCE Engineering Mechanics Conference (2003)
16. Kerschen, G., McFarland, D.M., Kowtko, J.J., Lee, Y.S., Bergman, L.A., Vakakis, A.F.: Experimental demonstration of transient resonance capture in a system of two coupled oscillators with essential stiffness nonlinearity. J. Sound Vib. **299**, 822–838 (2007)
17. Kozmin, A., Mikhlin, Y., Pierre, C.: Transient in a two-dof nonlinear system. Nonlinear Dyn. **51**, 141–154 (2008)
18. Lopez, G.: One-dimensional autonomous systems and dissipative systems. Ann. Phys. **251**, 372–383 (1996)
19. Lopez, G., Lopez, X.E., Hernandez, H.: One-dimensional relativistic dissipative system with constant force and its quantization. Int. J. Theor. Phys. **45**, 743–752 (2006)
20. Manevitch, L.I., Musienko, A.I.: Limiting phase trajectories and energy exchange between anharmonic oscillator and external force. Nonlinear Dyn. **58**, 633–642 (2009)
21. Manevitch, L.I., Kovaleva, A.S., Manevitch, E.L., Shepelev, D.S.: Limiting phase trajectories and non-stationary resonance oscillations of the duffing oscillator. Part 1. A non-dissipative oscillator. Commun. Nonlinear Sci. Numer. Simul. **16**, 1089–1097 (2011)
22. Manevitch, L.I., Kovaleva, A.S., Manevitch, E.L., Shepelev, D.S.: Limiting phase trajectories and nonstationary resonance oscillations of the duffing oscillator. Part 2. A dissipative oscillator. Commun. Nonlinear Sci. Numer. Simul. **16**, 1098–1105 (2011)
23. Matta, E., Stefano, A.D.: Robust design of mass-uncertain rolling-pendulum tmds for the seismic protection of buildings. Mech. Syst. Signal Process. **23**, 127–147 (2009)
24. Mikhlin, Y., Rudnyeva, G., Bunakova, T., Perepelkin, N.: Transient in 2-dof nonlinear systems. In: Modeling, Simulation and Control of Nonlinear Engineering Dynamical Systems, pp. 129–140 (2009)
25. Monroe, R.J.: Notes on transient dynamics of nonlinear oscillators. Tech. rep., Michigan State University (2011)
26. Monroe, R.J., Shaw, S.W.: Nonlinear transient dynamics of pendulum torsional vibration absorbers. In: Proceedings of the ASME 2011 International Design Engineering Technical Conferences & Computers and Information in Engineering Conference (IDETC/CIE) (2011)
27. Nayfeh, A.H., Mook, D.T.: Nonlinear Oscillations. Wiley, New York (1995)
28. Panagopoulos, P.N., Vakakis, A.F., Tsakirtzis, S.: Transient resonant interactions of finite linear chains with essentially nonlinear end attachments leading to passive energy pumping. Int. J. Solids Struct. **41**, 6505–6528 (2004)
29. Pradeep, R.G., Chandrasekar, V.K., Senthilvelan, M., Lakshmanan, M.: Nonstandard conserved hamiltonian structures in dissipative/damped systems: Nonlinear generalizations of damped harmonic oscillator. J. Math. Phys. **50** (2009)
30. Robinson, F.N.H.: Experimental observation of the large-amplitude solutions of Duffing's and related equations. IMA J. Appl. Math. **42**, 177–201 (1989)
31. Sato, H., Asada, K.: Laplace transform transient analysis of a non-linear system. J. Sound Vib. **121**, 473–479 (1988)
32. Shaw, S.W., Balachandran, B.: A review of nonlinear dynamics of mechanical systems in year 2008. J. Syst. Des. Dyn. **2**, 611–640 (2008)
33. Shaw, S.W., Geist, B.K.: Tuning for performance and stability in systems of nearly-tautochronic torsional vibration absorbers. J. Vib. Acoust. **132** (2010)
34. Shaw, S.W., Orlowski, M.B., Haddow, A.G.: Transient dynamics of centrifugal pendulum vibration absorbers. In: The 12th International Symposium on Transport Phenomenon and Dynamics of Rotating Machinery (2008)
35. Shaw, S.W., Schmitz, P.M., Haddow, A.G.: Dynamics of tautochronic pendulum vibration absorbers: Theory and experiment. J. Comput. Nonlinear Dyn. **1**, 283–293 (2006)
36. Struble, R.A., Yionoulis, S.M.: General perturbational solution of the harmonically forced duffing equation. Arch. Ration. Mech. Anal. **9**, 422–438 (1962)
37. Thomson, W.T., Dahleh, M.D.: Theory of Vibration with Applications. Prentice Hall, New York (1997)
38. Vakakis, A.F., Gendelman, O.V., Bergman, L.A., McFarland, D.M., Kerschen, G., Lee, Y.S.: Nonlinear Targeted Energy Transfer in Mechanical and Structural Systems: I and II. Springer, Berlin (2009)
39. Vakakis, A.F., Manevitch, L.I., Musienko, A.I., Kerschen, G., Bergman, L.A.: Transient dynamics of a dispersive elastic wave guide weakly coupled to an essentially nonlinear end attachment. Wave Motion **41**, 109–132 (2005)